

# STOCHASTIC MODELING OF MACROMOLECULAR MOTIONS THROUGH POST ARRAYS

*Yun-Bo Yi*

*Department of Mechanical and Materials Engineering, University of Denver, Denver, Colorado 80208, USA, E-mail: yyi2@du.edu*

*The dynamic motions of macromolecules through a microfluidic postarray system are simulated using a three-dimensional stochastic finite element approach. The effects of molecular conformation on the time for a macromolecule to move across the system are investigated. The analyses are first performed on disklike geometries and then extended to a representative carbonic anhydrase (CA) macromolecule model consisting of elastically deformable beam networks. The model predicts that smaller molecules typically take less time to pass through the post array, and that for stiff materials the time inversely increases with the aspect ratio of molecules due to the conformational changes in collisions between the molecules and the obstacles. In addition, the dynamic responses of molecules are highly stochastic. The work has potential applications in designing functional microfluidic devices for separation and purification of macromolecules such as plasmid DNA.*

**KEY WORDS:** *macromolecules, post arrays, stochastic modeling, finite element analysis*

## 1. INTRODUCTION

Exploring molecular propulsion mechanisms in fluidic devices for separation technology is of significant importance in biomedical applications such as gene therapy (Prazeres and Ferreira, 2004). In many applications, microfluidic channels are used to enhance molecular separation techniques by employing electrophoresis (Cole et al., 2000) or electroosmotic (Huang et al., 2002) phenomena to induce molecular movements in flows. Experimental results revealed that small molecules generally move faster than large ones in these devices (Chou et al., 1999; Kaji et al., 2004), making continuous sorting possible (Bakajin et al., 2001). By tuning the magnitude and intervals of the electric fields, the separation rates could be enhanced or optimized (Cole and Tellez, 2002). Han and Craighead (2000), on the other hand, demonstrated a method to create entropic traps for collecting a particle size range of molecules. This was successfully achieved by changes in macromolecular conformation via altering the channel dimension and utilizing a postarray system. These confinement channels separate DNA fragments of different size based on the physical mechanism that as the channel diameter approaches the size of a molecule, the channel walls can prohibit some molecular conformations (Turner et al., 2002; Cabodi et al., 2002). These limitations could result in a measurable force on the molecule (Foquet et al., 2002). Tuner et al. (2002) measured the magnitudes of such forces experimentally and reported a magnitude on the order of femto-Newtons. Therefore flow channels could be designed such that only those molecules within a specific length scale will have the necessary free energy to move through the system.

Traditionally molecular dynamics (MD) simulations (Mirny and Shakhnovich, 2001) have been the primary tools for modeling mechanical behaviors of molecules (Shea et al., 2001) and (Onuchic et al., 1997). However these techniques are computationally time prohibitive, and therefore limited to relatively small molecular lengths and short time scales. For large molecules such as DNA strands, although researchers reported DNA dynamics using MD (Jendreck et al., 2003), for long-time behaviors of DNA in a flow channel with post arrays, using an MD approach would generally be difficult.

One way to overcome the difficulty is to apply the computational homogenization theory, which was developed by Fish (2006) to bridge different scales in the general context of heterogeneous stochastic materials for both linear

and nonlinear solid mechanics problems (Fish and Fan, 2008; Yuan and Fish, 2008). More specifically, a multiscale computational procedure, which is compatible with conventional finite element code architectures such as those used in ABAQUS, can be developed to exploit the similarity between the engineering global-local design practice and multilevel approaches (Fish and Shek, 2000). This theory permits consideration of uncertainties in stochastic materials without exhausting the available computational resources (Fish and Wu, 2011). An adaptive strategy based on the finite element method can then be implemented to form an optimal model for predicting the mechanical behaviors of molecular systems.

In order to adopt this strategy, the detailed responses of individual molecules must first be explored. For many molecules composed of nucleotide subunits, they can be treated as small units bonded into long chains as done previously by Rzehak et al. (2000) and Hur and Shaqfeh (2001). Mechanically, this kind of chain network can always be modeled as an equivalent beam system (Berhan et al., 2004a) possessing either elastic or hyperelastic material properties (Berhan et al., 2004b; Yi et al., 2004). In view of this, although it would be difficult to simulate the motion of each individual atom in a macromolecule due to the sheer number of atoms, the problem can be simplified by modeling their subunits rather than individual atoms. For example, most therapeutic plasmid DNA in clinical trials contains approximately 5000 base pairs: a number that falls in the range of the concurrent computing technology. The potential energy stored in such a model can account for the entropic effects dominated in the interaction between molecules and the confinement when the channel size is comparable to the molecular diameter. Using this approach, the change of conformation and other mechanical behaviors of the molecules in confined channels can be simulated. Apparently, the required model parameters should be determined inversely from experiments.

Recently this idea was adopted by the author in modeling macromolecular motions in simple channels using two approaches: finite element discretization and probabilistic methods (Yi and Lengsfeld, 2006). As a proof of concept, the mechanical behavior of a CA molecule was studied, where the molecule was modeled as a beam network constructed by the backbone atoms. Each pair of the adjacent atoms formed an elastic beam that bears both axial and shear stresses. Molecular conformation and associated dynamic behaviors of the reconstructed molecule were investigated via two protocols: (1) compression of the molecule under a pair of parallel plates and (2) propagation of the molecule through a converging channel. The probabilistic simulation results along with the characteristic velocity profiles demonstrated the capability of this approach to capture physically relevant behaviors.

The preceding work was informative in that it revealed some fundamental features of molecular movement in confinement channels. However, the channel configuration proposed in the work is difficult to apply to practical devices, due to the fact that a flow channel with throat diameter close to the size of a single molecule will likely be blocked by the molecules themselves. The current research is a continued work following an analogous methodology. However, it targets investigating macromolecular movements in more realistic channels, in which the channel diameter is larger than the molecule scale and an array of post columns is incorporated to model the conformation changes. Adequate characterization of molecular behavior in confined channels through an efficient modeling tool in conjunction with future experiments will make possible the design of an integrated, functional system for separation of macromolecules of different types.

## 2. METHODS

### 2.1 Molecules Approximated as Circular or Elliptical Disks

Employing a mathematically simplified model to derive fundamental features of the problem of interest is always the first step in tackling a complicated physical process. The simplest model to study the dynamic responses of a molecule moving through a flow channel would be to utilize a two-dimensional geometry of either circular or elliptical shape for the molecule, as shown schematically in Fig. 1. Given a fixed channel design, various geometrical parameters may affect the system dynamics especially the time needed for the object to cross the device (let us define this quantity as “escape time” in the current study). Among these parameters, two are the most important: mean diameter and aspect ratio of the molecule. Elliptical disk is an ideal geometry in that only two variables are needed to describe its size and shape. In addition, the smooth boundary of an ellipse can avoid possible singularities in the solution and thus improve the numerical efficiency and accuracy.

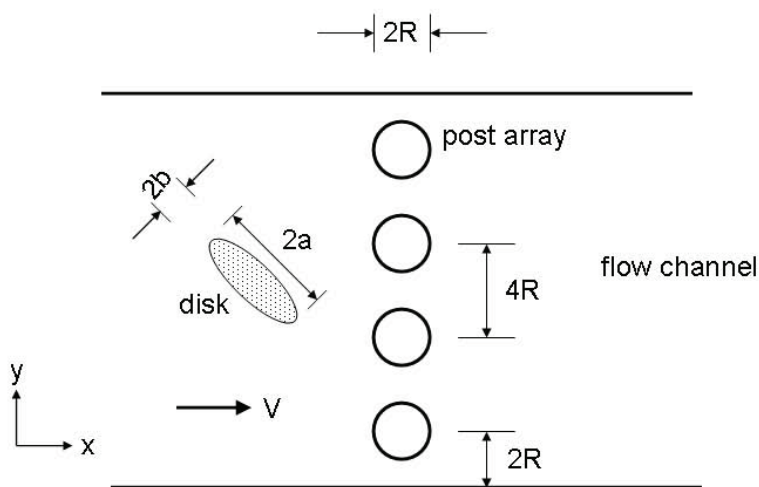


**FIG. 1:** Schematic of a flow channel and post array system with disk-shaped molecules.

The material properties, including elastic modulus and density, are also important. These parameters not only affect the numerical solutions of the problem but also change the convergence speed of the iteration process. Under some conditions, for example, when the loading speed is increased to a point at which the inertial effects dominate, the solution tends to localize and this will possibly initiate stress wave propagation in the structure. Although this phenomenon is not of interest in the present study, the computational speed will noticeably slow down. A set of simulation parameters (as shown in Table 1) close to those used in the author's previous work were used here to make the results consistent. Further, to simplify the analysis procedure, those material properties such as viscoelasticity, nonlinear behaviors, anisotropic properties, and interfacial Coulomb frictions are not considered in the present computational model. The methodologies developed in this research can be easily extended to these cases in the future.

When more than one disk is incorporated in the model (this should be more physically realistic since a number of molecules will likely move together in the channel and there are possible interactions between different molecules as well), we need to deal with multiple-body collision problems. This could be handled using rigid-body dynamics by assuming infinite elastic modulus. However, in more general situations, the molecular structures are flexible and the deformability in the material needs to be taken into consideration in the finite element simulation. In the present work, the simulation was realized using the commercial finite element code ABAQUS EXPLICIT since this software was designed to solve complicated contact problems as those involved in the present work. The finite element mesh was created using the general-purpose multiphysics simulation software COMSOL, and then imported to ABAQUS along with the appropriate boundary and loading conditions. The disks were propelled by the pressure drop in the channel. Although modeling the actual fluid flow in the problem would be ideal, numerically handling the fluid–solid interactions will be difficult in general. One way to circumvent the difficulties would be to assume steady flow conditions and use an equivalent force system to approximate the solid–fluid interactions. This is reasonable because of the Newtonian and laminar flows in microfluidic channels. In the present study the fluid part was simplified in such a way that the flow pressure acting on the disks was replaced by a body force equivalent to the hydraulic pressure drop

**TABLE 1:** Parameters used in the finite element analyses

Beam section diameter	Elastic modulus	Density	Initial velocity	Simulation time	Equivalent nodal force*
0.01 Å	$1.0 \times 10^{10}$ Pa	$1.0 \times 10^{-7}$ kg/mm <sup>3</sup>	100 Å/s	10.0 s	$1.0 \times 10^{-6}$ N

\*Note: This force is equivalent to the pressure drop due to the fluid flow.

in the channel. As a result, the disks behaved like a falling object subject to “gravity” in the direction of fluid flow and the “gravity constant” is proportional to the pressure drop correspondingly.

The frictionless contact condition was applied to the model by using a set of contact elements between the surfaces of the posts and the disks in contact. When more than one disk was involved, multiple contact pairs were defined. The interfacial contact changed both the linear and angular velocities of the disk and thus the disk would adjust its positions and orientations in the next time step. In some cases, the updated orientation allowed the disk to “squeeze” through the post array; in other cases, the angle between the major axis of the ellipse and the  $x$  direction was not large enough to allow the entire disk to move through. In the latter cases, the disk could possibly bounce back and then start a new attempt to squeeze through the posts. It is possible that the disk bounced for many times and thus it could have taken a long time for the disk to cross the post array at the end. Once the design of the post array is fixed, the probability for a circular disk to cross a post array within a fixed amount of time is determined by the size, initial velocity and elastic modulus of the disks. For ellipses, one more parameter, namely aspect ratio, can have an impact on this probability.

## 2.2 Dynamic Motions of Carbonic Anhydrase Across a Post Array

Modeling molecules using circular or elliptical disks can reveal some basic features of the problem especially when smaller molecules that have relatively inflexible structures are involved. However, for macromolecules with complex geometrical conformations their different portions may have varied flexibility and deformability. As a result, both the linear and angular velocities in the interior of a macromolecule may have substantially different values upon collisions with the array of posts and channel walls. In addition, it is evident that using a two-dimensional model to understand the molecular motions in three dimensions may be inappropriate in some circumstances. The dynamic responses of a macromolecule are therefore different from those of continuous, solid circles or ellipses and a direct modeling of the motion of molecules using detailed three-dimensional structure is therefore necessary.

CA (Carbonic Anhydrase II Mutant E117Q, Apo Form Huang et al., 1996) is an enzyme that catalyzes the hydration of carbon dioxide and the dehydration of bicarbonate. It has been found in all animals and photosynthesizing organisms. Compared to large molecules such as DNA, the size of a CA is much smaller and thus easier to model yet it is still categorized as a “macromolecule” Therefore it is ideal to use a CA molecule as a proof of concept for directly modeling three-dimensional molecular structure. In the present computational model, a CA molecule was approximated as a long chain of beams connected by the backbone carbon atoms, with each beam approximating a carbon-carbon bond, as shown in Fig. 2. Other atomic bonds in the molecules were not included in the model since

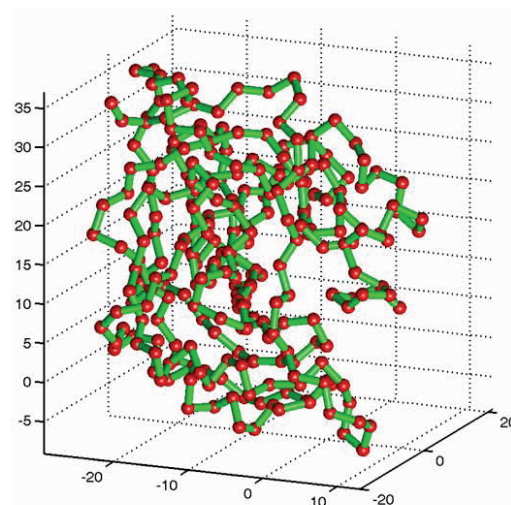


**FIG. 2:** A carbonic anhydrase (CA) molecule reconstructed as a deformable beam network by connecting the backbone carbon atoms. The axes represent the dimensions in the  $x$ ,  $y$  and  $z$  directions with the unit angstroms ( $\text{\AA}$ ).

their effects are believed negligible compared to the backbone bonds. The spatial coordinates of the carbon atoms were extracted from the macromolecular structure database that is available in the Protein Data Bank (RCSB PDB). The total number of the carbon atoms is 257 and therefore the number of the elastic beams is 256. The motion of the entire beam network was simulated in the interior of a simple flow channel equipped with an array of equisized cylindrical microposts.

An initial linear velocity was assigned to the beam network to enable the network to move toward the post array. The structure underwent elastic deformation during its dynamic collisions with the channel walls and post surfaces. The frictionless contact condition was assumed by using a set of gap elements between the contact nodes on the beams and the rigid surfaces of walls and posts. Therefore the nodal contact scheme was employed and the penetration of the contact nodes was examined during each time step of numerical iteration. Although the frictionless contact was assumed in the system, a loss in the kinetic energy of the translational motion associated with the mean linear velocities was anticipated. This is because some kinetic energy could be transformed into angular motion during the collisions against the boundaries. Nevertheless, there was no frictional loss and the total energy and momentum should always be conserved.

Similar to the preceding disk models, the posts here were uniformly distributed in the middle of the flow field. The molecular motion was propelled by the pressure drop in the fluid. When a collision occurred, there was elastic deformation in the molecular structure and the altered shape of the molecule could change the pressure field in the fluid. This in turn affected the forces acting on the molecule, resulting in a solid–fluid interaction in the system. This interaction could be more intense than in the solid disk model due to the fact that a beam network is generally more flexible to allow more severe deformation. However, for convenience, the problem was still simplified in a way that the flow field remained the same regardless of the solid–fluid interaction. Further, as in the disk model, the force acting on the molecule was replaced by a body force equivalent to the hydraulic pressure drop in the flow. The calculated body force was then converted to concentrated forces acting on the discrete finite element nodes that represent carbon atoms. These are reasonable assumptions in the conditions when the sizes of the posts and the molecule are much smaller than the size of the channel.

Two types of molecular configuration were under investigation. The first type was the standard CA molecule (let us denote it as “molecule  $\alpha$ ”) and the second type was an artificially altered CA molecule with its length doubled in the flow direction and shortened by half in the other direction (let us denote it as “molecule  $\beta$ ”), as shown in Fig. 3. The length in the third dimension (i.e. along the axes of posts) remains the same. In this way the same volume (thus the same amount of mass given the same density) was maintained in the two molecules to minimize the total number of variables in the problem. By studying the dynamic behaviors of these two molecules, it is possible to understand the behaviors of other macromolecules as well, including those with substantial variations in conformation such as the linear forms and supercoiled forms of DNA, because of the geometrical similarities in these molecules. The simulation was also run in the commercial finite element code ABAQUS. The nodal displacement results were obtained by averaging the values over all the beam members in the structure and therefore they were considered as

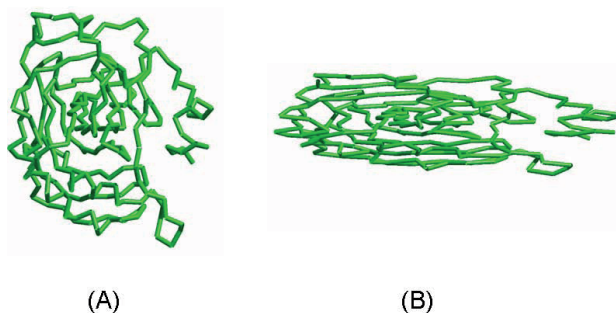


**FIG. 3:** Two molecular conformations in comparison: (A) original CA molecule and (B) an altered CA molecule by stretching one dimension and shortening the other dimension while keeping the volume the same.

mean displacements at the mass centers. Other dynamic quantities including velocity and acceleration can also be evaluated by taking the derivatives of displacement.

### 2.3 Probabilistic Analysis

In both disk and beam models, the randomness in the parameters of molecules must be taken into consideration and the simulation results should be interpreted as probabilistic. When the positions of the posts are fixed, the main uncertainties in the problem will be induced by the randomness in the spatial locations and the conformational orientations of the molecules when they enter the inlet of the channel. If all the possible values of random variables were considered, the computation would be extremely cumbersome. Fortunately, one can take advantage of the geometrical symmetries in the problem: for the post array, only one column of posts is needed and the behaviors of molecules across multiple columns of posts can be deduced from the results using a single post column. Further, when the post number is sufficiently large, the boundary effects will be negligible and the behaviors of a molecule will almost remain the same when it moves through the posts located at different  $y$  positions. Therefore in the same column array two arbitrary posts (e.g. two adjacent posts in the middle) were selected and the molecule was initially positioned somewhere between the two posts, as shown in Fig. 1. This significantly reduced the total number of random variables defining the molecular spatial location. For molecular orientation, randomness can be realized by applying a rotation matrix on the nodal coordinates. In the case of ellipses, only one variable is needed to define the orientation angle of the object; in the case of CA molecules or other general three-dimensional geometries, three independent angles are required to define the orientation.

In general, we have

$$\begin{bmatrix} u - x_0 \\ v - y_0 \\ w - z_0 \end{bmatrix} = \Omega \begin{bmatrix} x - x_0 \\ y - y_0 \\ z - z_0 \end{bmatrix} \quad (1)$$

where  $x$ ,  $y$ , and  $z$  represent the centroidal coordinates of the molecule;  $x$ ,  $y$ ,  $z$  are the original nodal positions of the nodes;  $u$ ,  $v$  and  $w$  are the nodal positions after the rotation; and  $\Omega$  is the rotation matrix. Mathematically, the three-dimensional space rotations about the  $x$ ,  $y$  and  $z$  axes require the following operations:

$$\Omega_x(\alpha) = \begin{bmatrix} 1 & 0 & 0 \\ 0 & \cos \alpha & \sin \alpha \\ 0 & -\sin \alpha & \cos \alpha \end{bmatrix}, \quad \Omega_y(\beta) = \begin{bmatrix} \cos \beta & 0 & -\sin \beta \\ 0 & 1 & 0 \\ \sin \beta & 0 & \cos \beta \end{bmatrix}, \quad \Omega_z(\gamma) = \begin{bmatrix} \cos \gamma & \sin \gamma & 0 \\ -\sin \gamma & \cos \gamma & 0 \\ 0 & 0 & 1 \end{bmatrix}, \quad (2)$$

where  $\alpha$ ,  $\beta$ , and  $\gamma$  are the rotational angles about the three axes, respectively. Because an arbitrary rotation can always be decomposed into individual rotations about each of the three axes, one can write a rotation matrix as

$$\Omega = \Omega_x(\alpha)\Omega_y(\beta)\Omega_z(\gamma) \quad (3)$$

The orientation of the tri-axes of a threedimensional random system can be described in a Euler system by the azimuthal and rotational angles with a uniform distribution and the polar angle with a probability density function biased toward the equator (Yi and Lengsfeld, 2006). Finally, the effects of randomness in the above variables can be estimated using a set of equally spaced, fixed values of parameters. The computed results will then be averaged over the entire range of variation.

## 3. RESULTS AND DISCUSSION

### 3.1 Circular Disks

Figure 4 shows the simulation results related to the time for circular disks to cross the post array. The time was measured between the two instants when a disk crossed the locations immediate to the left and right sides of the post array (along the  $x$  direction). The distances between these locations and the center points of the posts are equal to the post diameter to ensure there is enough initial clearance between the disk and the posts. In addition, normalized results

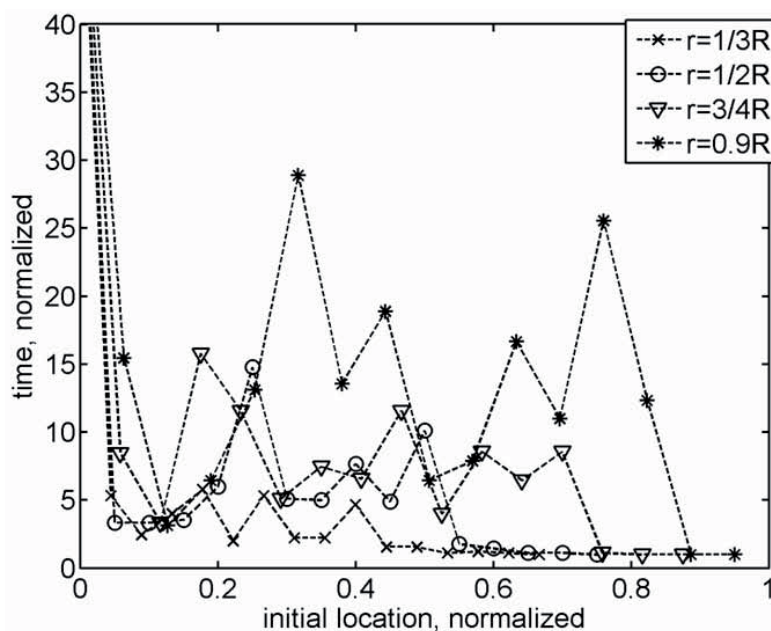


**FIG. 4:** Time taken by a circular disk to cross a single array of posts. It is normalized against the time with no posts present. The initial location is the  $y$  distance between the center location of the disk and its nearest post location normalized by  $2R$ , the post diameter.

are presented in the figure; the time has been normalized against the time taken by a disk to move through the system without colliding with the posts. The distance has been normalized by the post diameter. Finite element simulations were run by using several different disk radii for the purpose of comparison.

The results show that the relationship between the time and distance traveled by the disks is highly nonlinear. When the disk was aligned with the post center, it kept bouncing above the post surface and hence the time for the disk to pass the post array was infinite. When the disk was shifted away from the centerline slightly, the pathways of the disk were still blocked by the posts. However, after bouncing back and forth for a number of times, the trajectory of the disk eventually fell into the gaps between the posts and resulted in a finite escape time. On the far left ends of the curves in Fig. 1, it can be seen that the escape time was reduced drastically when the initial locations increased from zero. However, in some incidents, the disk could not “squeeze” through the post array even after many times of collision. Therefore the curves exhibit some local peaks and the locations of these peaks seem to be randomly determined by the disk diameter. When the disks were moved further away from the centerlines of the posts, they might be able to freely pass through the gaps without collisions as long as the initial  $y$  distance between the disk and the posts is greater than the sum of the disk and the post radii. As a consequence, all the curves converge to unit values at the right ends.

These curves reveal that the disk diameter has significant effects on the time needed for the disks to travel through the post array. For example, on average the escape time for  $r = 0.9R$  was five times greater than that for  $r = 1/3R$ , where  $r$  is the disk radius and  $R$  is the post radius. In fact, when  $r > R$  and neglecting deformability, the disk will be trapped in between the posts and it will never be able to escape. A smaller disk will certainly have less chance to make collisions with the posts and the time is therefore reduced. The same reason gave rise to the result that the curve for a smaller  $r$  converged faster to unity than a larger  $r$ .

On the other hand, comparisons between two scenarios  $r = 1/2R$  and  $r = 3/4R$  do not show pronounced differences in terms of the mean escape time. This implies a possibly nonlinear relationship between the disk diameter and the escape time to some extent.

### 3.2 Elliptical Disks

Incorporation of noncircular disks in the simulation increases degrees of freedom in the model and it can change the probability of collision between the disks and the posts. Figure 5 shows the impact of aspect ratio on the escape time. The lengths of the major and minor axes of ellipse  $a$  and  $b$  were determined by the formula  $ab = R^2$  so that a constant area was maintained for all the disks, where  $R$  is the post radius. The aspect ratio of the disk is defined as  $\varepsilon = a/b$ . The orientation angle took evenly spaced values between zero and  $2\pi$  to approximate a random distribution. The simulation results were then averaged over these situations and the mean values were computed.

A comparison of the three curves in the figure reveals that an increase in the aspect ratio reduced the overall escape time, implying it was easier for a longer molecule to move through the system. This is because the minor axis length was smaller for a disk of larger aspect ratio and the probability of part of the disk falling inside the gap increased. From Fig. 5 it is seen that the mean escape time for circular disks was about three times that for elliptical disks of aspect ratio  $\varepsilon = 5$ . Again, the locations of the peaks in the curves were randomly distributed and determined by the geometry and initial location of the disk. The randomness also reflects the statistical noise induced by the varied orientation angle of the disk. On the other hand, although the mean time was reduced for a high aspect ratio, the variation was also reduced. Consequently, at some locations it could take less time for a disk of low aspect ratio to cross the post array. For example, normalized time was 3.07 at initial location 0.13 for aspect ratio  $\varepsilon = 1$  whereas normalized time was 1.09 at initial location 0.13 for  $\varepsilon = 5$ .

Figure 6 shows a sequence of simulation results when multiple circles and ellipses were coexistent in the model. In addition, multiple columns of posts were involved for a direct simulation of the entire post array. The radii of the circular disks as well as the spacing between the posts were set to the post radius. Therefore the circular disks could not even pass the first post column. The aspect ratio of the ellipses is 2 and it can be seen that all of the ellipses successfully crossed the system at the end, although it took relatively longer time for some of them. This result has confirmed that less time is needed for solid disks of higher aspect ratio to cross a postarray system.

### 3.3 CA Molecules

The Monte Carlo simulation results using a CA molecule are presented in Fig. 7. The molecule was initially positioned in the upstream and the distance between the mass center of the molecule and the center point of the adjacent post was the mean molecular diameter to avoid the molecule from touching the post at the very beginning.

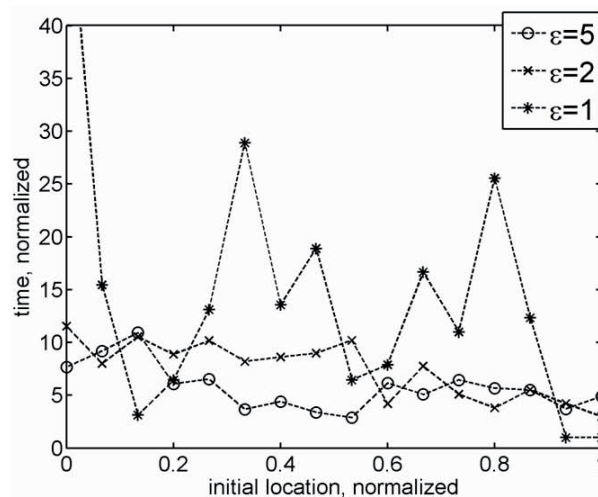


**FIG. 5:** Time taken by an elliptical disk to cross a single array of posts. It is normalized against the time with no posts present. The initial location is the  $y$  distance between the center location of the disk and its nearest post location normalized by  $2R$ , the post diameter.



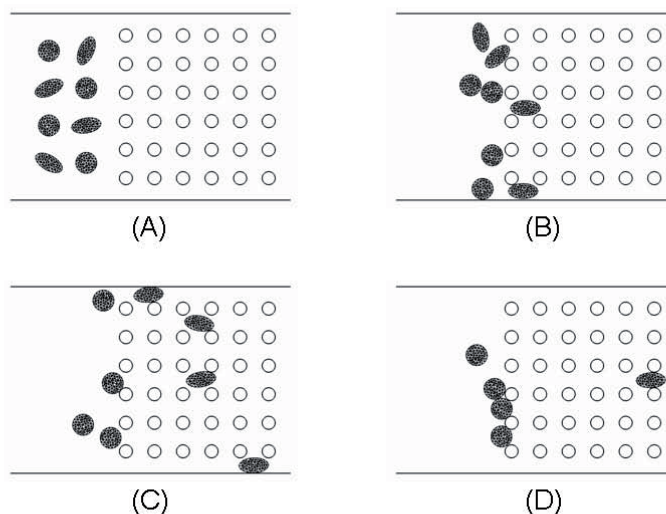


**FIG. 6:** Finite element analysis using a mix of elliptical and circular objects indicates that the postarray design favors elongated objects to move across the system. (A)–(D) The simulation results in time sequence.

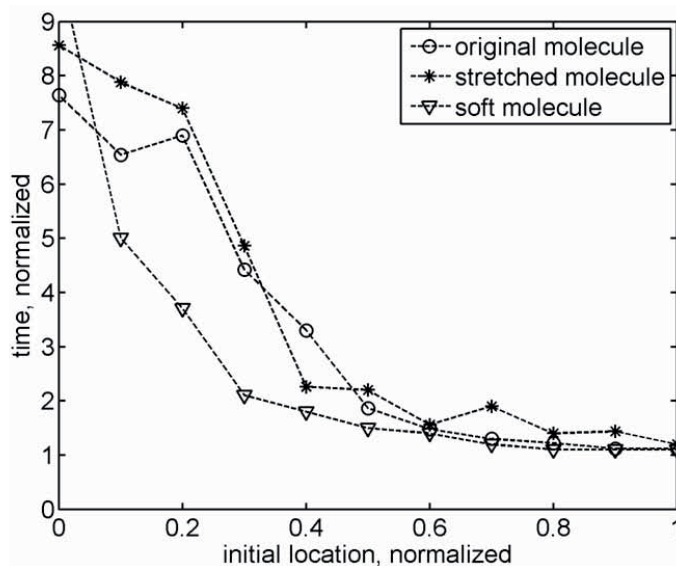


**FIG. 7:** Time taken by a CA molecule to cross a single array of posts. It is normalized against the time with no posts present. The “initial location” represents the  $y$  distance between the mass center of the molecule and the centerpoint of its nearest post normalized by  $2R$ , the post diameter.

In the figure, we can clearly see that the time increased monotonically with distance (i.e., when the mass center moved away from the centerline of the post into the gaps between the posts). When the molecule was aligned with the post, the dimensionless time was approximately between 8 and 10. By contrast, the time was close to unity when the molecule was aligned with the gap. This is due to the reduced probability of collision against the posts in the latter case, which was similar to the results of solid disks. However, it is seen from the figure that the short and elongated molecules did not show much difference in terms of the elapsed time: the two curves are almost parallel with slight

variations in each of them. This observation is apparently different from those of solid disks. The reason lies in the flexibility of the molecular structure. A beam network reconstructed from the backbone atoms is much easier to deform during collisions in comparison with solid ellipses or circles, and it can change its own conformation substantially at some points of the process, as seen in Fig. 8. In some circumstances, the molecule could even wrap around the post and stretched itself under the body force. This behavior resulted in an extensive collision time, which differs from the solid disk models. The randomness in the change of conformation during collisions was partly cancelled by the randomness induced by the differences in the original aspect ratios of geometry. Consequently, only minor disagreement in the dynamic responses has been observed for the two molecules. It is unclear whether the same conclusion will hold when the aspect ratio increases to a relatively larger value. Nevertheless it is expected that the discrepancies would be small if there were any. Furthermore, because of the same reason, a molecule modeled by a beam network with a diameter larger than a post can also “squeeze” through the system by dynamically changing its geometrical shape during collisions.

Rigidity of the beam system can alter the collision time and thus affect the computational results. Considering two extreme cases in which the modulus approaches infinity and zero, the macromolecule will behave like a rigid disk in the former case and a soft string or cord in the latter case. When the elastic modulus is sufficiently large, the escape time will be close to that of an ellipse or ellipsoid of the same geometrical aspect ratio; when the modulus is sufficiently small, the time will approach unity because the molecule can deform into an arbitrary shape and the post system will not impose any mechanical constraints on the molecule’s rigidbody motion. Figure 7 has verified this hypothesis: that is, it took less time for a softer molecule to cross the post array. Please note that the elastic modulus had been reduced by ten times for the softer molecule compared to the control molecule.

#### 4. CONCLUSIONS

The mechanical motions of macromolecules in a flow channel through a uniform postarray system were tentatively simulated using two computational models: a simplified solid disk model and a representative, realistic macromolecule carbonic anhydrase. Finite element analyses were performed to investigate the effects of several primary parameters, including disk aspect ratio and elastic modulus, on the time needed for a molecule to travel through the post array. The numerical models predicted that smaller molecules generally take less time to cross the system, which is consistent with the conclusions drawn from the fundamental physics and dynamics. But the most striking conclusion is for

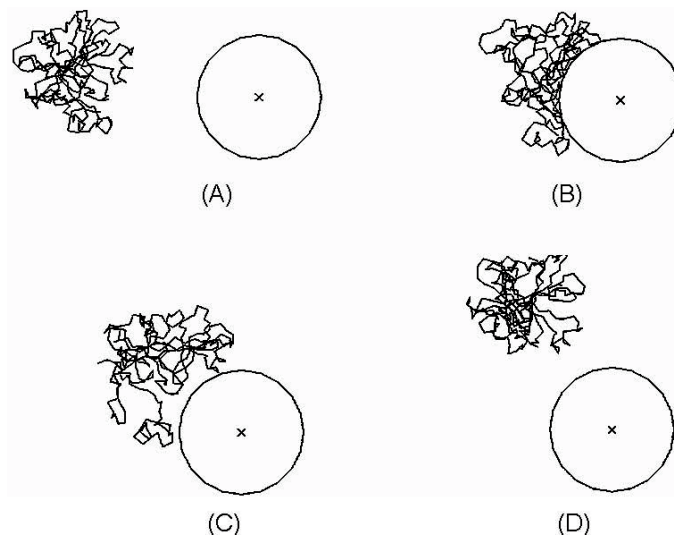


**FIG. 8:** Changes in the morphology of a CA molecule during its collision against a rigid post. (A)–(D) are finite element simulation results in the time sequence.

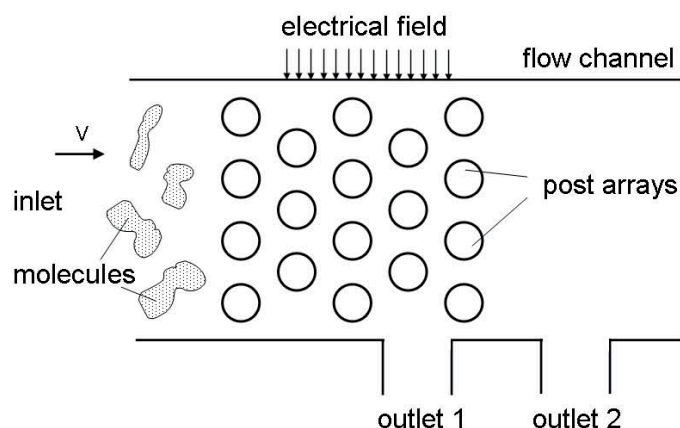


**FIG. 9:** A conceptual fluidic channel for macromolecular separation. Electrostatic forces are applied to induce vertical velocities on the molecules.

a relatively stiff structure, the time inversely changes with the aspect ratio; whereas for a soft, flexible molecule, the escape time (or mean velocity) could be independent of the geometrical shape of the molecule. In addition, the dynamic responses of a molecule are highly stochastic due to various initial and boundary conditions. Future studies will focus on the interactions between fluid and solid surfaces to incorporate the dynamic changes of the fluid pressure acting on the molecule, so that the relevant physical processes can be better understood and predicted. This work has potential applications in design and optimization of a functional microfluidic device for molecular separation and purification in biomedical engineering, as shown schematically in Fig. 9. The simulation methodologies proposed in the current work can provide useful information on efficiency, parameter optimization, and intermolecular interactions therefore laying the groundwork for practical implementation.

## REFERENCES

- Bakajin, O., Duke, T. A. J., Tegenfeldt, J., Chou, C. F., Chan, S. S., Austin, R. H., and Cox, E. C., Separation of 100-kilobase DNA molecules in 10 seconds, *Anal. Chem.*, vol. **73**, pp. 6053–6056, 2001.
- Berhan, L., Yi, Y. B., Sastry, A. M., Munoz, E., Selvidge, M., and Baughman, R., Mechanical properties of nanotube sheets: Alterations in joint morphology and achievable moduli in manufacturable materials, *J. Appl. Phys.*, vol. **95**, pp. 4335–4345, 2004a.
- Berhan, L., Yi, Y. B., and Sastry, A. M., Effect of nanorope waviness on the effective moduli of nanotube sheets, *J. Appl. Phys.*, vol. **95**, pp. 5027–5034, 2004b.
- Cabodi, M., Turner, S. W. P., and Craighead, H. G., Entropic recoil separation of long DNA molecules, *Anal. Chem.*, vol. **74**, pp. 5169–5174, 2002.
- Chou, C. F., Bakajin, O., Turner, S. W. P., Duke, T. A. J., Chan, S. S., Cox, E. C., Craighead, H. G., and Austin, R. H., Sorting by diffusion: An asymmetric obstacle course for continuous molecular separation, *Proc. Natl. Acad. Sci. U.S.A.*, vol. **96**, pp. 13762–13765, 1999.
- Cole, K. D., Tellez, C. M., and Blakesley, R. W., *Electrophoresis*, vol. **21**, pp. 1010–1017, 2000.
- Cole, K. D. and Tellez, C. M., Separation of large circular DNA by electrophoresis in agarose gels, *Biotechnol. Prog.*, vol. **18**, pp. 82–87, 2002.
- Fish, J. and Shek, K., Multiscale analysis of composite materials and structures, *Compos. Sci. Technol.*, vol. **60**, pp. 2547–2556, 2000.
- Fish, J., Bridging the scales in nano engineering and science, *J. Nanopart. Res.*, vol. **8**, pp. 577–594, 2006.

- Fish, J. and Fan, R., Mathematical homogenization of nonperiodic heterogeneous media subjected to large deformation transient loading, *Int. J. Numer. Methods Eng.*, vol. **76**, pp. 1044–1064, 2008.
- Fish, J. and Wu, W., A nonintrusive stochastic multiscale solver, *Int. J. Numer. Methods Eng.*, vol. **88**, pp. 862–879, 2011.
- Foquet, M., Korfach, J., Zipfel, W., Webb, W. W., and Craighead, H. G., DNA fragment sizing by single molecule detection in submicrometer-sized closed fluidic channels, *Anal. Chem.*, vol. **74**, pp. 1415–1422, 2002.
- Han, J. and Craighead, H. G., Separation of long DNA molecules in a microfabricated entropic trap array, *Science*, vol. **288**, pp. 1026–1029, 2000.
- Huang, C. C., Lesburg, C. A., Kiefer, L. L., Fierke, C. A., and Christianson, D. W., Reversal of the hydrogen bond to zinc ligand histidine-119 dramatically diminishes catalysis and enhances metal equilibration kinetics in carbonic anhydrase II, *Biochemistry*, vol. **35**, pp. 3439–3446, 1996.
- Huang, L. R., Tegenfeldt, J. O., and Kraeft, J. A., DNA prism for high-speed continuous fractionation of large DNA molecules, *Nature Biotechnol.*, vol. **20**, pp. 1048–1051, 2002.
- Hur, J. S. and Shaqfeh, E. S. G., Dynamics of dilute and semidilute DNA solutions in the start-up of shear flow, *J. Rheol.*, vol. **45**, pp. 421–450, 2001.
- Jendrejack, R. M., Dimalanta, E. T., Schwartz, D. C., Graham, M. D., and de Pablo, J. J., DNA dynamics in a microchannel, *Phys. Rev. Lett.*, vol. **91**, p. 038102, 2003.
- Kaji, N., Tezuka, Y., Takamura, Y., Ueda, M., Nishimoto, T., Nakanishi, H., Horiike, Y., and Baba, Y., Separation of long DNA molecules by quartz nanopillar chips under a direct current electric field, *Anal. Chem.*, vol. **76**, pp. 15–22, 2004.
- Mirny, L. and Shakhnovich, E., Protein folding theory: From lattice to all-atom models, *Annu. Rev. Biophys. Biomol. Struct.*, vol. **30**, pp. 361–396, 2001.
- Onuchic, J. N., Lutheyschulzen, Z., and Wolynes, P. G., Theory of protein folding: The energy landscape perspective, *Annu. Rev. Phys. Chem.*, vol. **48**, pp. 545–600, 1997.
- Prazeres, D. M. F. and Ferreira, G. N. M., Design of flow sheets for the recovery and purification of plasmids for gene therapy and DNA vaccination, *Chem. Eng. Proc.*, vol. **43**, pp. 609–624, 2004.
- Rzehak, R., Kromen, W., Kawakatsu, T., and Zimmerman, W., Deformation of a tethered polymer in uniform flow, *Eur. Phys. J. E*, vol. **2**, pp. 3–30, 2000.
- Shea, J. E. and Brooks, C. L., From folding theories to folding proteins: A review and assessment of simulation studies of protein folding and unfolding, *Annu. Rev. Phys. Chem.*, vol. **52**, pp. 499–535, 2001.
- Turner, S. W. P., Cabodi, M., and Craighead, H. G., Confinement-induced entropic recoil of single DNA molecules in a nanofluidic structure *Phys. Rev. Lett.*, vol. **88**, p. 128103, 2002.
- Yi, Y. B., Berhan, L., and Sastry, A. M., Statistical geometry of random fibrous networks, revisited: Waviness, dimensionality, and percolation, *J. Appl. Phys.*, vol. **96**, pp. 1318–1327, 2004.
- Yi, Y. B. and Lengsfeld, C. S., Mechanical modeling of carbonic anhydrase motion in simple channels, *J. Appl. Phys.*, vol. **100**, p. 014701, 2006.
- Yuan, Z. and Fish, J., Toward realization of computational homogenization in practice, *Int. J. Numer. Methods Eng.*, vol. **73**, pp. 361–380, 2008.